APPLIED PHYCOLOGY
2023, VOL. 5, NO. 1, 1–11
https://doi.org/10.1080/26388081.2023.2280928

Eliciting specialized metabolites from marine microalgae using abiotic stress

Alison H. Hughes and Katherine R. Duncan

University of Strathclyde, Strathclyde Institute of Pharmacy and Biomedical Sciences, Glasgow, UK

ABSTRACT

Advanced mass spectrometry and molecular networking techniques have led to an increase in the discovery of novel metabolites from bacteria and fungi. However, a systematic approach to exploring the metabolite profiles of microalgae in response to stress has not been performed. Unlocking the chemical potential of microalgae could provide further biotechnology applications in nutraceutical, biofuel, and cosmetic industries. This study explored the changes in metabolite production of strains of the three microalgae *Dunaliella primolecta, Nannochloropsis oculata*, and *Phaeodactylum tricornutum* cultured under varying nitrate, NaCl, salinity and pH conditions. A total of 2284 metabolites were detected across all strains and conditions, with 49% of those metabolites specific to cultures grown under stress (i.e., not present in the control). From comparison with 33 libraries of mass spectral data, only five metabolites were identified, stressing the need for more open-access natural product databases specifically focused on microalgae.

ARTICLE HISTORY
Received 20 May 2023
Accepted 2 November 2023

KEYWORDS
Microalgae; molecular networking; metabolites; nitrate; salinity; pH

Introduction

Microalgae have piqued the interest of researchers due to the abundance of reported bioactivities and industrial applications, including biofuels, cosmetics, and nutraceuticals. However, we still have little understanding about the chemical space occupied by microalgal metabolites. As such, the discovery of metabolites from eukaryotic microalgae remains dismally low. The 2023 Marine Natural Products report detailed the discovery of 1425 new metabolites from marine organisms in 2021 (Carroll, Copp, Davis, Keyzers, & Prinsep, 2023). According to this report, 18 metabolites were discovered from dinoflagellates – primarily from toxic *Karenia* species (Hort, Abadie, Arnich, Bottein, & Amzil, 2021) and 14 from cyanobacteria. This is compared to 212 bacterial and 607 fungal marine natural products. Like many other microorganisms, microalgae have the molecular machinery to produce a plethora of diverse metabolites that are not always detected using standard laboratory culture methods. Various strategies have been used to unlock the chemical potential of microorganisms, including genome mining, genetic engineering, and synthetic biology. Whilst these strategies have been successful in bacteria and filamentous fungi, the size and complexity of microalgal genomes still present challenges. However, advances in sequencing and molecular toolkits have been made in recent years, including the use of Clustered Regularly Interspaced Short Palindromic Repeats/CRISPR-Associated Protein 9 (CRISPR/Cas9) systems to edit genes in *Phaeodactylum tricornutum* (Nymark, Sharma, Sparstad, Bones, & Winge, 2016), genetic engineering of *Nannochloropsis oceanica* for increased polyunsaturated fatty acid production (Poliner et al., 2018), and the addition of introns into *Chlamydomonas* genes to improve transgene expression (Baier, Wichmann, Kruse, & Lauersen, 2018). Although this is an exciting time for microalgal molecular biology, progress is slow and expensive (Fu, Nelson, Mystikou, Daakour, & Salehi-Ashtiani, 2019). As such, simpler, untargeted approaches to unlocking the chemical potential of microalgae are often used, including the elicitation of metabolites by manipulating culture conditions.

One such way of driving the production of diverse metabolites is the One Strain Many Compounds (OSMAC) approach (Bjorn Bode, Bethe, Hofs, & Zeeck, 2002), which has proven that small changes in growth conditions can lead to the production of specialized metabolites that would otherwise remain undiscovered when grown under standard laboratory conditions. This approach also has ecological relevance as some metabolites will be triggered in response to specific stress. When the chlorophyte *Dunaliella salina* is subjected to salt stress (up to 5 M), the level of reactive oxygen species, such as hydrogen peroxide, increases (Xi, Kong, & Chi, 2021). To counteract this, the alga produces the powerful antioxidant β-carotene in large quantities (up to 10% dry weight) (Xu & Harvey, 2019).

CONTACT Katherine R. Duncan katherine.duncan@strath.ac.uk
Supplemental data for this article can be accessed online at https://doi.org/10.1080/26388081.2023.2280928

This natural response by *D. salina* has been exploited by the biotechnology industry to produce natural β-carotene. Salt concentration is a common stress used for marine microorganisms as they have metabolic mechanisms in place for osmoregulation in response to fluctuating salinity encountered in their native environment. Salinity in the oceans varies from 30 psu in the Arctic Ocean to 37 psu in the North Atlantic Ocean (Atlantic Ocean 2021; Pacific Ocean | Depth 2021), and these values shift according to climate, seasons, and vicinity to fresh water such as rivers and glaciers. Therefore, marine organisms must be able to adapt to the osmotic pressure created by shifting salinities, as well as the change in mineral and nutrient concentrations of the seawater. Due to the complexity of natural seawater, synthetic seawaters such as Instant Ocean® and Aquil synthetic seawater (Morel, Rueter, Anderson, & Guillard, 1979) can also be used, however sodium chloride (NaCl) is often used as a proxy for studying the effects of salinity on metabolite production.

Natural seawater also contains dissolved nutrients which are required for all organisms in the ocean to survive. Phytoplankton requires a specific ratio, known as the Redfield ratio, of 106:16:1 carbon, nitrogen, and phosphorus, respectively (Tett, Droop, & Heaney, 1985). Nitrogen sources that include ammonium (NH_4^+), nitrate (NO_3), nitrite (NO_2^-), and urea (NH_4N_2O) have been studied for their bioavailability and both nitrogen source and nitrogen concentrations have been used in the OSMAC approach to elicit production of specific metabolites (Chaffin, Bridgeman, & Bade, 2013; Li et al., 2016). Culturing *Nannochloropsis* sp. under nitrogen-starved conditions has been shown to increase triacylglycerol content by almost 3% (Ahamad et al., 2022). Not only is this an important discovery in our search for sustainable biofuels that do not interfere with food security, but it has wider ecological importance as our lakes and oceans undergo eutrophication from fertilizer runoff, sewage disposal, and climate change (Smayda, 2008). Eutrophication leads to the explosion of harmful algal blooms in both freshwater and marine habitats leading to hypoxic conditions and poisoning of animals through the production of harmful algal toxins (Béchemin, Grzebyk, Hachame, Hummert, & Maestrini, 1999). Coinciding with eutrophication of waters is the acidification of the oceans which also leads to harmful algal blooms, often referred to as red tides (Falkenberg et al., 2020). The reduction in the pH of oceans has been shown to reduce the buffering capacity of the ocean, increasing carbonate mineral dissolution and hydrogen sulphide oxidation (Cai et al., 2017). It has also been reported that certain microalgal toxins (known as M-toxins) that cause paralytic shellfish poisoning are actually more stable and less likely to degrade under lower pH values which could result in harmful algal blooms having a longer lasting impact as a result of ocean acidification (Che, Ding, Qiu, Ji, & Li, 2020). On the other hand, the effect of low pH has also been used to increase the production of beneficial microalgal metabolites in controlled settings. Culturing *Haematococcus pluvialis* at pH 4 significantly reduces the fungal contaminant *Paraphysoderma sedebokerensis*. Combining the acidic pH with nitrogen deficiency led to a 141-fold increase in astaxanthin production in *H. pluvialis* cultures (Hwang, Choi, & Sim, 2019).

After conducting a literature review on the ecological and biotechnological potential of abiotic stress on microalgae, salinity (both sodium chloride and Aquil synthetic seawater concentrations), nitrate concentration, and pH were chosen as stresses for further investigation. In order to systematically evaluate the effect of individual abiotic stresses on marine microalgae, three strains (*Nannochloropsis oculata* CCAP 849/1, *Dunaliella primolecta* CCAP 11/34, and *Phaeodactylum tricornutum* CCAP 1055/15) were grown under varying concentrations of sodium chloride (deplete, 0 g l^{-1}; low, 12 g l^{-1}; control 24 g l^{-1}; and high 36 g l^{-1}), Aquil synthetic seawater (low, 4.3 ppt; control, 43 ppt; and high, 86 ppt), sodium nitrate (low, 8.82×10^{-5} M; control, 8.82×10^{-4} M; and high, 8.82×10^{-3} M), and varying pH (low pH 4, control pH 7.6, and high pH 10). Comparative metabolomics was then used to compare the effects of these abiotic parameters on produced microalgal chemistry.

Methods

Algal culture

Stock cultures of *Dunaliella primolecta* CCAP 11/34, *Nannochloropsis oculata* CCAP 849/1, and *Phaeodactylum tricornutum* CCAP 1055/15 were maintained in f/2 medium (Guillard, 1975) and modified Aquil synthetic seawater (Cai et al., 2017) (no boric acid, sodium fluoride, or strontium chloride hexahydrate) at 20°C in a static Panasonic MIR-154-PE incubator with a 12-h light:dark cycle and 75 µmol m^{-2} s^{-1} illumination. Stock cultures were used to inoculate 100 ml experimental cultures in triplicate (Table 1) which were maintained under identical conditions. Growth was monitored using absorbance at 600 nm until cultures reached stationary phase.

Table 1. Culture conditions used for each stress.

	NaCl (g/l^{-1})	Salinity (Aquil concentration, ppt)*	Sodium nitrate concentration (M)	pH
Deplete	0			
Low	12	4.3	8.82×10^{-5}	4 (buffered with 1 M sodium citrate)
Control	24	43	8.82×10^{-4}	7.6 (not buffered)
High	36	86	8.82×10^{-3}	10 (buffered with 1 M TRIS)

*Varying concentrations of Aquil synthetic seawater were prepared by adjusting the concentration of individual salts used to prepare the media, with the exception of sodium hydrogen carbonate that was maintained at 0.5 g/L across all conditions.

Extraction

HP-20 diaion resin (Alfa Aesar) was activated using ethyl acetate, and 5% w/v of dried resin was added to cultures and agitated overnight at 160 rpm. Once cultures reached stationary phase, cells were pelleted using a centrifuge (4200 rpm, 30 min, Thermo Scientific Heraeus Megafuge 40 R) and the supernatant was discarded. Frozen cell pellets (−80°C) and HP-20 resin were lyophilized before being extracted overnight with 50 mL of ethyl acetate (120 rpm) and dried *in vacuo*.

LC-MS/MS analysis

Extracts were prepared at 1 mg in 2:2:1 acetonitrile: methanol:water and run in triplicate on a Thermo UltiMate™ 3000 UPLC. A 10 µl aliquot was injected onto a Kinetex C18 reversed-phase column (100 × 2.1 mm, 1.7 µm; Phenomenex, Cheshire, UK) connected to the UPLC with a flow of 300 µl min^{-1}. A binary gradient of solvent A (Millipore water with 0.1% formic acid) and solvent B (acetonitrile with 0.1% formic acid) was used, as follows: 0.5 min at 5% B, 8 min gradient from 5% to 50%, 2 min gradient from 50% to 99% B, 2 min at 99% B, 1 min gradient from 99% to 5% B, 2 min at 5% B. Extracts were analysed using a Thermo Scientific Q-Exactive in positive mode ESI, with a mass range of 150–1500 *m/z*, and a resolution of 35,000. Data-dependent MS2 scans were performed on the 1st, 2nd, and 3rd most intense peaks using CID with a resolution of 17,500. The ion spray voltage was set to 4.2 kV, the capillary temperature was 310°C.

Classical molecular networking

Converted mzML spectral files were uploaded to the GNPS (Wang et al., 2016) platform and the medium data present was selected. The precursor ion mass tolerance was set at 2 Da and the fragment ion tolerance was 0.5 Da. The minimum pairs cosine value was 0.7, network topK was 10, maximum connected component size of 100, minimum matched fragment ions was set to 3, minimum cluster size of 2, and minimum peak intensity was 1×10^4. The same parameters were used for the library search and solvent blanks were filtered from the data before networking. The resultant GraphML file and cluster table were imported to Cytoscape v3.8.2 for annotation (Shannon et al., 2003).

Results

Growth of Dunaliella primolecta, Nannochloropsis oculata *and* Phaeodactylum tricornutum *under varying abiotic conditions*

Lowering the concentration of nitrate tenfold to 8.82×10^{-5} M decreased the growth of all three strains (Fig 1). This decrease was significant for *N. oculata* ($p = 0.015$) and *P. tricornutum* ($P = 0.009$) (Supplementary table S1) but due to the spread of measurements for the *D. primolecta* replicates, it is unclear just how much of an impact low nitrate concentration had on this strain. For each strain, growing it under 0 g l^{-1} NaCl resulted in a significant decrease in growth as expected, as each of these strains were isolated from a marine environment and maintained in saline conditions. The specific growth rates of *D. salina* remained unaffected under growth at 12 g l^{-1}, 24 g l^{-1}, and 36 g l^{-1} NaCl (average µ = 4.34, 5.05, and 4.27, respectively) (Supplementary table S1) compared to growth under varying salinity which was significantly reduced for both low (4.3 ppt) and high (86 ppt) conditions. The specific growth rate of *N. oculata* almost doubled when grown in 36 g l^{-1} NaCl from 14.75 to 26.26 per day. This increase was not as large when *N. oculata* was grown under high salinity. Conversely, growth of the diatom *P. tricornutum* decreased by 71% when grown under high NaCl but only decreased by 13% when grown under high salinity. Finally, *P. tricornutum* was the only strain to be significantly affected by pH stress with average specific growth rates of 11.26 per day for pH 4, 13.38 per day for pH 7.6, and 7.94 per day for pH 10. In contrast, growth of *N. oculata* remained unaffected by acidic or basic pH conditions, and surprisingly, *D. primolecta* grew significantly better under acidic conditions ($p = 0.04$).

Metabolite profiles of Dunaliella primolecta, Nannochloropsis oculata *and* Phaeodactylum tricornutum *under varying abiotic conditions*

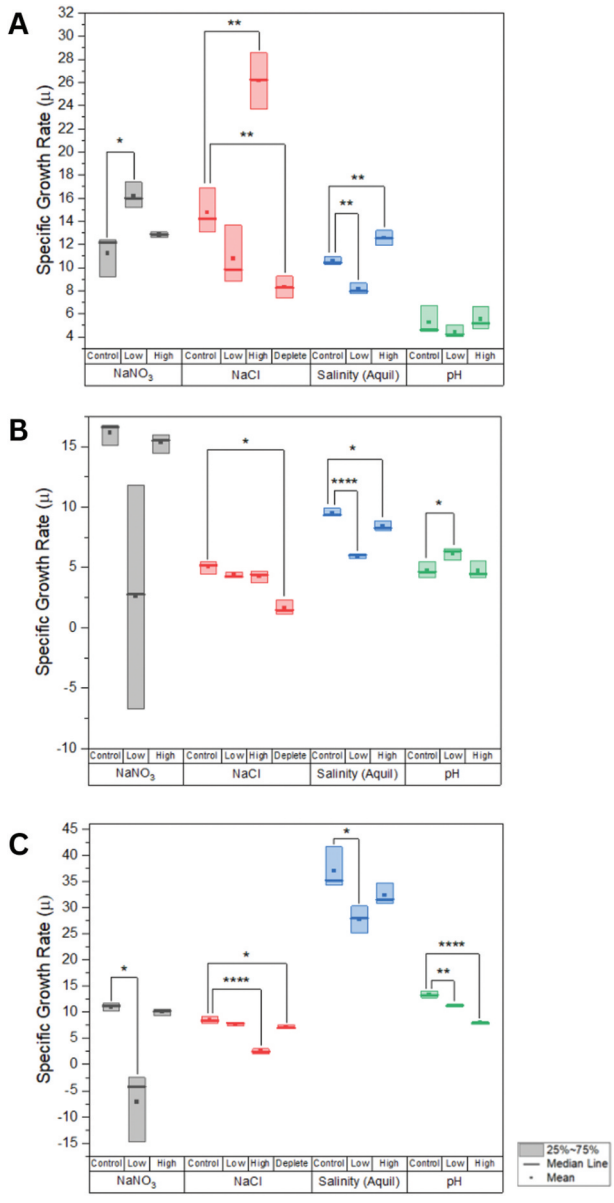

Figure 1. Box plots summarizing the growth rates of (A) *Nannochloropsis oculata*, (B) *Dunaliella primolecta*, and (C) *Phaeodactylum tricornutum* grown under varying conditions with box plots showing the 25–75% range, median values as thick lines and mean values as solid squares. Conditions are as follows: $NaNO_3$ (grey); control (8.82×10^{-4} M), low (8.82×10^{-5} M), high (8.82×10^{-3} M); NaCl (red); control (24 g l^{-1}), low (12 g l^{-1}), high (36 g l^{-1}), deplete (0 g l^{-1}); salinity (blue); control (43 ppt), low (4.3 ppt), high (86 ppt); and pH (green); control (7.6), low (4), high (10). p-values are based on a t-test between condition and control for each stress.

A molecular network of extracts from the three strains grown under each abiotic condition in triplicate comprised 2284 nodes, of which 51.2% were shared between at least two of the three strains (SI Figure S1). However, there were still distinct differences in the chemical profiles of these strains, with 24.1% (550) of features only found in *P. tricornutum* extracts, 17.3% (391) of features unique to *D. primolecta*, and 7.4% (169) of features distinct from *N. oculata* extracts (Fig 2). Not only did each strain have a set of distinct features, but so did each stress. Focusing on features that were only produced in response to stress (i.e., NaCl, salinity, nitrate, or pH) revealed that 49% of features were only produced by strains grown under a particular stress. 22.8% of features were only produced in response to salinity stress, 17.1% in response to nitrate stress, 7.7% in response to NaCl stress, and 1.4% in response to pH stress (Fig 2). This is aligned with the effect seen on the growth of these organisms.

From the overview molecular network (SI Supplementary figure S1), salinity had the greatest effect on metabolite production with 22.8% of features detected from microalgal extracts from salinity stress. Of those features, 17.9–23.6% of metabolites were only produced under low salinity conditions (Fig 3). In total, 6.6–17.1% of metabolites were only produced under deplete NaCl and 4.4–10.8% of metabolites were only produced under low NaCl conditions. In fact, the spread of metabolites across each condition was similar for each strain. High salinity and NaCl concentration had a much smaller effect on metabolite production (3.6–5.4% for salinity and 2.9–6.3% for NaCl), showing that hypoosmotic stress had a greater influence on metabolite production than hyperosmotic stress (Fig 3). A notable difference across strains was that of *D. primolecta* grown under deplete NaCl, which stimulated the production of 191 (17.1%) metabolites that were not found in the other conditions. The poor growth and large change in metabolism further support the inference that *Dunaliella* spp. are obligate marine microalgae.

Varying nitrate concentrations also had a large impact on the metabolite profiles with 17.1% of metabolites only detected when strains were grown under nitrate stress. Of those features, 9.1–11.3% of metabolites were only produced under low nitrate conditions compared with 14.1–15.4% of metabolites detected in extracts from high nitrate (8.82×10^{-3} M) cultures. As with salinity, the distribution of metabolites across control, low, and high conditions is similar for all three strains (Fig 3).

For cultures grown under varying pH, only 1.4% of metabolites were produced specifically under pH stress. Again, the distribution of metabolites according to each condition was very similar for all strains with 6.1–11.8% only detected under high pH conditions, 6.1–8.0% only detected in control samples, and 7.3–8.2% of features only detected under low pH conditions. *D. primolecta* had a higher specific growth rate under acidic (low pH) conditions and this did correlate with a slightly higher (8.2% compared to 7.3% and 7.4%) number of metabolites detected for *D. primolecta* compared to the other two strains.

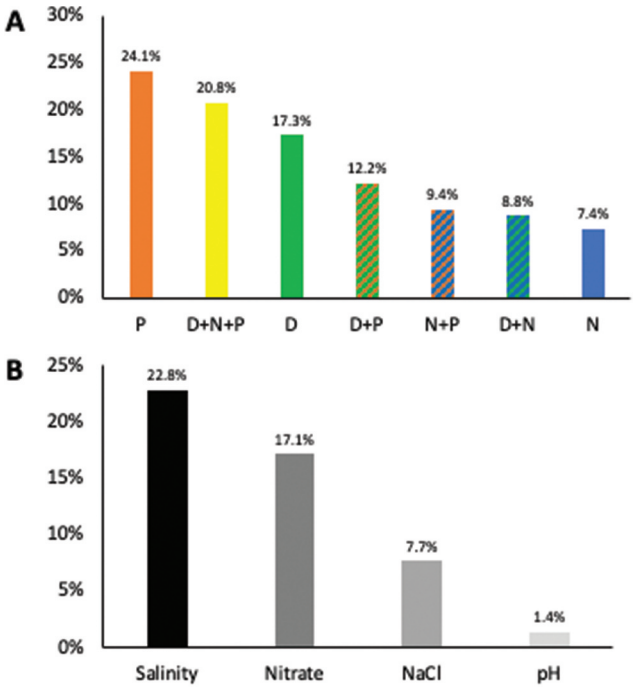

Figure 2. (A) bar chart showing the distribution of MS/MS features across strains: *P* = *Phaeodactylum tricornutum*, orange; D = *Dunaliella primolecta*, green; *N* = *Nannochloropsis oculata*, blue; D+P = features shared between *D. primolecta* and *P. tricornutum*, green and orange stripes, D+N = features shared between *D. primolecta* and *N. oculata*, green and blue stripes, N+P = features shared between *N. oculata* and *P. tricornutum*, blue and orange stripes, D+N+P = features shared between all three strains, yellow. (B) bar chart of the percentage of MS/MS features only detected in response to specific stresses; varying salinity (Aquil synthetic seawater), nitrate concentrations, NaCl concentrations, and pH. The percentages of total MS/MS features are listed above each bar.

Salinity and NaCl

From the salinity molecular network (Supplementary fig. S2), 2749 features were detected, 28% of which were from the media and solvent controls. Individual networks were created for each strain with the highest number of features detected for *P. tricornutum* at 701, followed by *D. primolecta* with 584 features, and *N. oculata* with 348 (Supplementary fig. S3). The only metabolites identified through comparison with the GNPS libraries were monopalmitolein and 1-octadecanamide (stearamide) which were found in all strains grown under all salinity and NaCl conditions. The lack of matches to previously discovered metabolites made dereplication and putative identification of derivatives a very difficult (or impossible) task.

Metabolites that were only detected from a specific strain clustered together into molecular families and this could be seen in the salinity and NaCl molecular networks. For example, Fig 4A shows that 24 of the 35 metabolites in this molecular family were only detected in samples from *P. tricornutum* (orange). Of those 35, 25 were only found under low salinity conditions, with the majority of metabolites having medium–high molecular weight (721.382–1177.67 *m/z*). Another molecular family (Fig 4B) of structurally similar (cosine score > 0.7) medium–high molecular weight metabolites (672.406–1233.76 *m/z*) were only produced by *P. tricornutum* under low salinity, and another molecular family of seven low molecular weight metabolites (372.738–781.545 *m/z*) were only produced under high salinity. This was also observed for *N. oculata* (Fig 4C) with another molecular family of high molecular weight metabolites (833.472–2284.49 *m/z*) only being detected for *N. oculata* grown under low salinity conditions. This trend is not as clear for *D. primolecta*, however, there were some small molecular families with three or four members that were only produced under low salinity conditions (Fig 4D).

Nitrate

The nitrate molecular network (Supplementary fig. S4) had the highest overall number of 4982 features detected, with 12.6% from media and solvent controls. Individual networks were created for each strain with 1003 features detected for *P. tricornutum*, 843 for *D. primolecta*, and 667 for *N. oculata* (Supplementary fig. S5). Only one molecular family predominantly comprised metabolites (913.507–1221.68 *m/z*) solely detected when *D. primolecta* was cultured under high nitrate (Fig 5A). A few other molecular families showed examples of metabolites that were only produced in response to high or low nitrate in all three strains. For example, Fig 5B shows three metabolites with parent masses 635.385, 679.277, and 784.491 *m/z* which were detected in samples from all three strains under low nitrate conditions. Similarly, Fig 5C shows a molecular family with four metabolites (477.234, 563.27, 649.308, and 838.408 *m/z*, yellow triangles) which were produced by all three strains under high nitrate.

pH

The pH network showed a total of 1197 features were detected, with 48% coming from the media and solvent controls (Supplementary fig. S6). *P. tricornutum* had the highest number of features detected with 335, followed by *D. primolecta* with 284, and *N. oculata* with 184 (Supplementary fig. S7). Monopalmitolein and 9,12-octadecadien-1-ol were the only metabolites identified through matching with the GNPS spectral libraries and were detected in all strains grown under all conditions.

As seen in the nitrate network, there were a lot of metabolites shared between two or more of the strains (25.7%). Although changes in nitrate concentration

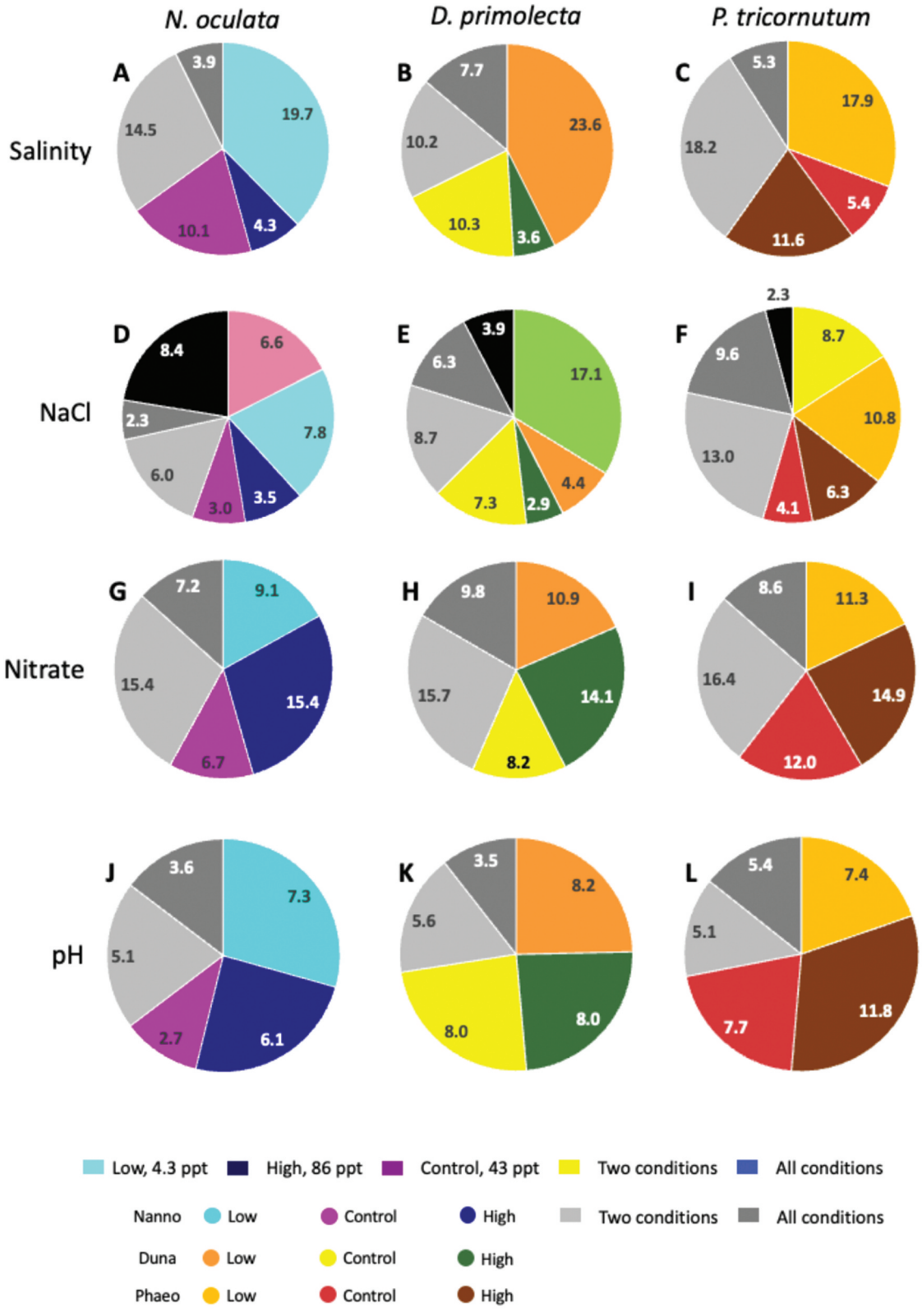

Figure 3. Pie charts illustrating the distribution of MS/MS features as percentages (given in figure) for all three strains under all four stresses: (A) *Nannochloropsis oculata* grown under varying salinity, (B) *Dunaliella primolecta* grown under varying salinity, (C) *Phaeodactylum tricornutum* grown under varying salinity, (D) *N. oculata* grown under varying NaCl concentrations, (E) *Dunaliella primolecta* grown under varying NaCl concentrations, (F) *P. tricornutum* grown under varying NaCl concentrations, (G) *N. oculata* grown under varying nitrate concentrations, (H) *D. primolecta* grown under varying nitrate concentrations, (I) *P. tricornutum* grown under varying nitrate concentrations, (J) *N. oculata* grown under varying pH, (K) *D. primolecta* grown under varying pH, and (L) *P. tricornutum* grown under varying pH.

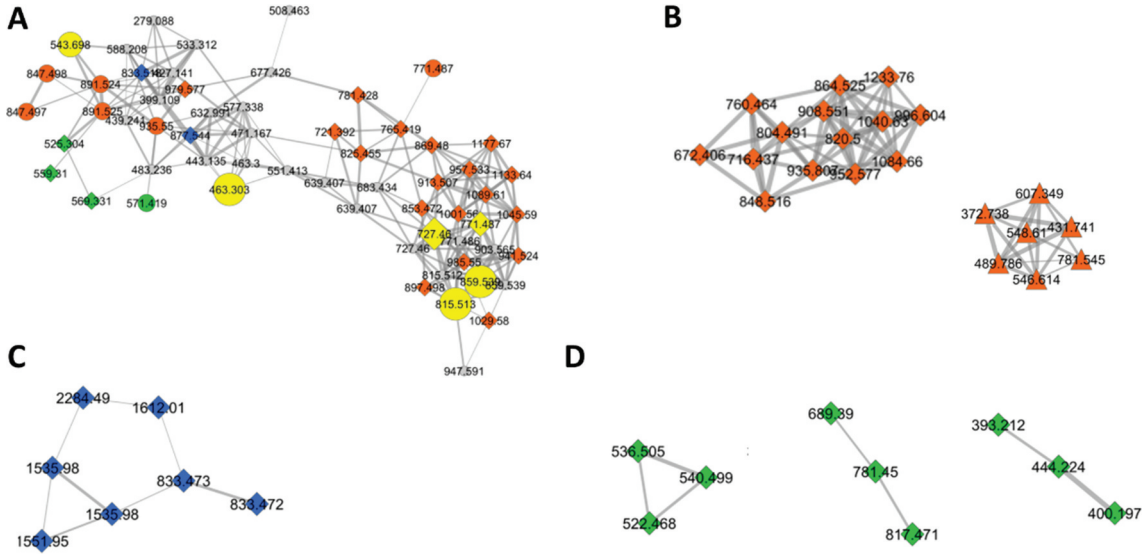

Figure 4. Examples of molecular families detected under specific conditions: (A) metabolites only produced by *Phaeodactylum tricornutum* (orange), *Nannochloropsis oculata* (blue) and *Dunaliella primolecta* (green) under low (diamonds) or high (triangles) salinity conditions. Metabolites in orange are only produced by *P. tricornutum* with diamonds representing metabolites only produced under low salinity, (B) metabolites only produced by *P. tricornutum* (orange) under low salinity (diamonds) or high salinity (triangles), (C) molecular family produced in response to low salinity by *N. oculata*, (D) molecular families produced in response to low salinity by *D. primolecta*.

seemed to affect metabolites shared by all three strains, changes in pH affected metabolites that were strain-specific. In fact, only one metabolite with a parent mass of 764.577 *m/z* was detected in samples produced by all three strains in response to acidic conditions (Fig 6A). Although most metabolites impacted by pH stress were strain-specific, these metabolites clustered together in molecular families which made it difficult to define trends in the data. For example, Fig 6B shows a molecular family of 19 metabolites, six of which were present in control samples from all strains, one (473.435 *m/z*) which was only found in samples from all strains grown in basic conditions and five metabolites that were strain-specific under basic conditions. Two of those metabolites were specific to *N. oculata* (487.414 and 349.31 *m/z*), another two were specific to *P. tricornutum* (543.44, 884.712 *m/z*) and one to *D. primolecta* (445.403 *m/z*). This molecular family also contained a sub-cluster of five metabolites

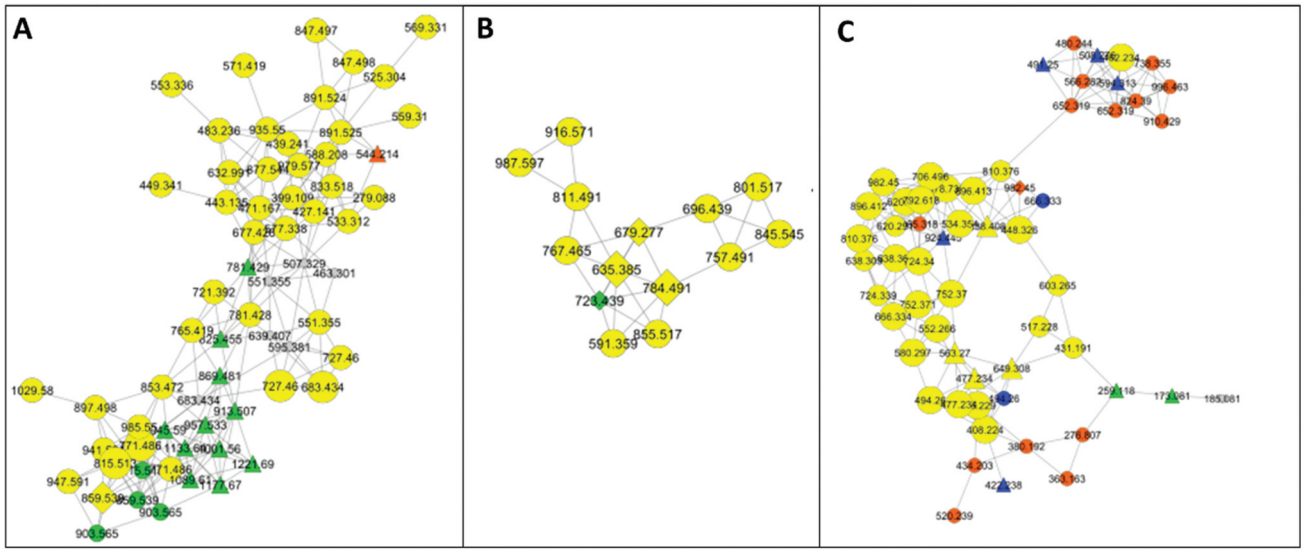

Figure 5. Metabolites only produced by *Phaeodactylum tricornutum* (orange), *Nannochloropsis oculata* (blue) and *Dunaliella primolecta* (green), or by multiple strains (yellow) under low (diamonds) or high (triangles) nitrate conditions.

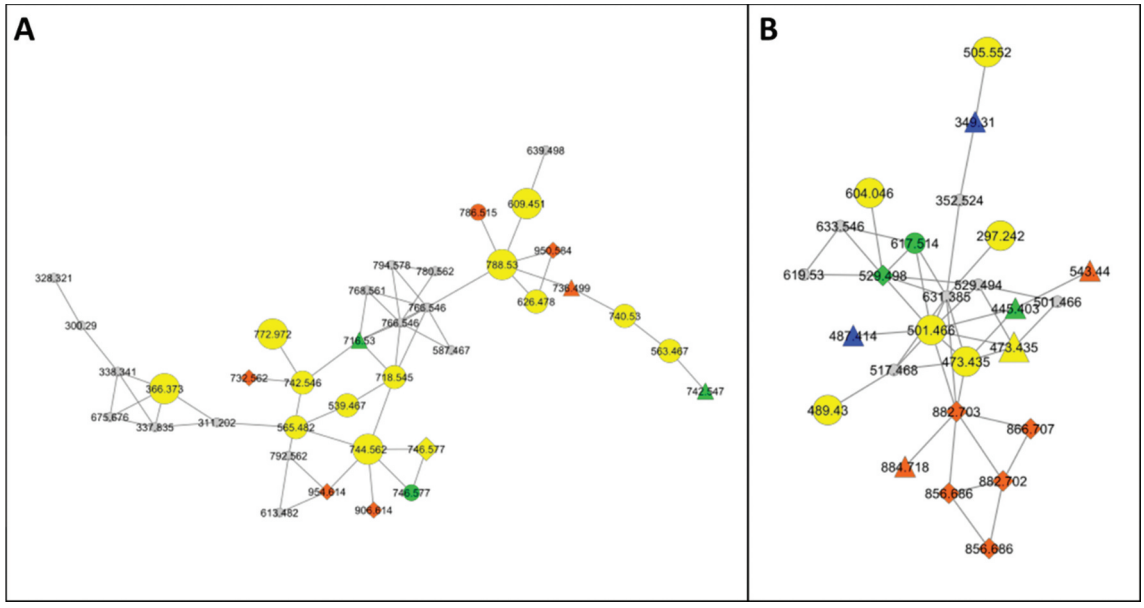

Figure 6. Metabolites only produced by *Phaeodactylum tricornutum* (orange), *Nannochloropsis oculata* (blue) and *Dunaliella primolecta* (green), or by multiple strains (yellow) under acidic (diamonds) or basic (triangles) pH conditions.

detected from *P. tricornutum* acidic samples and had much higher molecular weights than the rest of the molecular family, with a range 856.686–886.707 *m/z*. It can be postulated that some of the features detected in these networks were degradation products due to the instability of certain classes of natural products under basic or acidic conditions.

Discussion

From this analysis, there was a general trend that a decrease in growth resulted in an increase in metabolite production. Renauld & Parry (1994) observed that total lipid content increased with salinity (from 10 to 35 ppt) for *Nannochloropsis oculata*, with *cis*-9-hexadecanoic acid 16:1 (*n*-7) increasing up to 24.1% of total fatty acids when grown under 35 ppt salinity. However, this was coupled with a significant reduction in the specific growth rate of *N. oculata* at 35 ppt (Renaud & Parry, 1994). Another study which used homology-based proteomics observed that under hypersaline (3 M NaCl) conditions, *D. primolecta* increased production of enzymes key to the Calvin cycles and regulating protein biosynthesis (Liska, Shevchenko, Pick, & Katz, 2004). This is believed to contribute to the organism's tolerance of hypersaline environments and could explain the variation in metabolite profile under low or deplete NaCl conditions when these metabolic pathways may be suppressed in favour of other pathways that will protect the cell from hyposaline conditions. In these two studies, hypersaline and high salinity were defined differently. In Renauld & Parry (1994), 35 ppt is equivalent to 0.6 M NaCl whilst the proteomics study defined 3 M NaCl as hypersaline. This makes comparison of results across studies very difficult. It also brings into question whether "high" and "low" conditions could be strain-specific. *Dunaliella* spp. are known to be halotolerant and *D. salina* is grown commercially in media with up to 5 M NaCl to maximize β-carotene. On the other hand, 0.6 M NaCl was sufficient to cause stress to *N. oculata* resulting in reduced growth and increased total fatty acid content. In conflict with this result, the specific growth rate of *N. oculata* CCAP 849/1 in this study almost doubled when grown under 0.62 M NaCl. This variation in defining high versus low conditions, and the response of individual strains to these conditions makes systematic investigations difficult to achieve and comparison to literature almost impossible.

Perhaps wider transcriptomic analyses could provide a solution to this problem and using microarrays would allow this to be done in a systematic and high-throughput way. Nagappan et al. (2020) published a thorough review on the physiological changes in microalgae in response to nitrogen starvation which included metabolomic, transcriptomic, proteomic, and chemical analyses from across the literature. This review illustrated the complexity of this area of research as nitrogen deprivation affected the production of chlorophyll, carbohydrates, carotenoids, lipids, and biomass, as well as altering the regulation of the Calvin cycle, glycolysis, the pentose phosphate pathway, and photosynthesis. It is undeniable that the OSMAC approach has led to the commercialization of high-value products from microalgae, such as β-carotene and astaxanthin,

which globally are worth US$155 million (2015) and US $770 (expected by 2024) (Mehar, Mudliar, Shekh, & Shekh, 2019). However, our fundamental understanding of how stress triggers the production of these – and other – useful metabolites remains poor. Its relevance to natural ecosystems and the environment requires much more research, especially as anthropogenic climate change continues to cause extreme weather events, eutrophication, ocean acidification, and global warming (Teuma, Sanz-Luque, Guieysse, & Plouviez, 2023).

The development of tools such as MZmine (Pluskal, Castillo, Villar-Briones, & Orešič, 2010), MS2LDA (Wandy et al., 2018), GNPS (Wang et al., 2016), and DEREPLICATOR (Ernst et al., 2019) have revolutionized the metabolomics field as they provide open-access and streamlined methods of analysing, visualizing, and annotating MS2 data. The GNPS ecosystem allows networks of structurally similar metabolites to be created and screened against 33 libraries of compounds. One downfall of this screening is that GNPS contains libraries such as MassBank (Horai et al., 2010) and the Institute of Standards and Technology (NIST) databases which also contain synthetic molecules not found in nature. Due to the paywall behind natural product libraries such as MarinLit (MarinLit, 2021), AntiBase (AntiBase, 2021), and Dictionary of Natural Products (Dunkel, 2006), they are not included in the GNPS ecosystem. In fact, only 2.5% of known natural products are contained in the GNPS libraries and this does not include any algal databases. This lack of available natural product and specifically, algal natural products libraries, makes annotation and dereplication a frustrating and unfruitful endeavour.

From the analysis above of 2284 metabolites only five metabolites were identified using GNPS libraries: monopalmitolein, 1-octadecanamine, hexanedioic acid, 13-keto-9Z,11E-octadecadienoic acid, and 9,12-octadecadien-1-ol. Gaining meaningful information from large MS2 datasets without the aid of dereplication requires the use of expensive instrumentation such as NMR and HPLC which give more detailed structural information and aid in isolation of metabolites, respectively. Even using NMR to guide the isolation of metabolites through HPLC can result in the isolation of known metabolites which is a huge loss of money and time when researchers are working within strict grant budgets and timeframes. One method to aid in the prioritization of metabolites from molecular networking is coupling this mass spectral data with bioactivity data. The bioactivity-based molecular networking platform was developed in 2018 and led to the discovery of new antiviral metabolites from the well-studied plant *Euphorbia dendroides* (Nothias et al., 2018). Since then, a database of *Euphorbia* metabolites was created and implemented into the MolNetEnhancer framework (Ernst et al., 2019) through Mass2Motifs (Wandy et al., 2018).

The work of Aldholmi et al. (2022) illustrates the importance of using a combination of growth stress and molecular networking to identify microalgal metabolites of importance. They tried many methods of culturing *Euglena gracilis* including autotrophic conditions and the use of epigenetic modifiers. It was only when they altered the nitrogen source that they were able to observe new metabolites, euglenatides A-E, with anti-fungal and anticancer activity. After isolating and characterizing the new metabolites, they performed molecular networking on the crude extracts and discovered a molecular family of over 40 euglenatide-like molecules (Aldholmi et al., 2022) As more metabolites from microalgae are discovered and characterized, more meaningful data can be obtained from molecular networking and thus lead to an explosion in discovery of high-value metabolites from these ecologically important organisms.

Our results on nitrate are interesting from an ecological point of view as eutrophication has seen an increase of nitrate in the oceans causing increased growth of microalgae (algal blooms). However, the effect of these increased nitrate levels on the metabolism of these organisms and how this may impact the food chain remains underexplored. It is remarkable that the high nitrate concentration had such an impact on metabolite production in our strains and this result could be important for understanding how eutrophication affects the aquatic food chain. It has been shown that high nitrogen and phosphorus levels lead to more blooms of toxic microalgae and cyanobacteria, but their effects on non-toxic or non-bloom forming microalgae require further investigation.

Disclosure statement

No potential conflict of interest was reported by the author(s).

Funding

This work was supported by the Industrial Biotechnology Innovation Centre.

ORCID

Katherine R. Duncan http://orcid.org/0000-0002-3670-4849

References

Ahamad, T. S., Brindhadevi, K., Krishnan, R., Phuong, T. N., Alharbi, S. A., Chinnathambi, A., & Mathimani, T. (2022).

Invivo detection of triacylglycerols through Nile red staining and quantification of fatty acids in hyper lipid producer *Nannochloropsis* sp. cultured under adequate nitrogen and deficient nitrogen condition. *Fuel*, *322*, 124179. doi:10.1016/j.fuel.2022.124179

Aldholmi, M., Ahmad, R., Carretero-Molina, D., Pérez-Victoria, I., Martín, J., and Ganesan, A. (2022). Euglenatides, potent antiproliferative cyclic peptides isolated from the freshwater photosynthetic microalga *Euglena gracilis*. *Angewandte Chemie International Edition Engl*, *61*, e202203175. doi:10.1002/anie.202203175

AntiBase. (2021, 07 05) A bioinformatics tool for natural product databases | chemoinformatics databases. Retrieved from https://omictools.com/antibase-tool

Atlantic Ocean | Definition, Temperature, Weather, & Facts. (2021). Retrieved from https://www.britannica.com/place/Atlantic-Ocean

Baier, T., Wichmann, J., Kruse, O., & Lauersen, K. J. (2018). Intron-containing algal transgenes mediate efficient recombinant gene expression in the green microalga *Chlamydomonas reinhardtii*. *Nucleic Acids Research*, *46*, 6909–6919. doi:10.1093/nar/gky532

Béchemin, C., Grzebyk, D., Hachame, F., Hummert, C., & Maestrini, S. (1999). Effect of different nitrogen/phosphorus nutrient ratios on the toxin content in *Alexandrium minutum*. *Aquatic Microbial Ecology: International Journal*, *20*, 157–165. doi:10.3354/ame020157

Bjorn Bode, H.; Bethe, B.; Hofs, R.; Zeeck, A. (2002). Big effects from small changes: Possible ways to explore Nature's chemical diversity. *ChemBiochem*, *3*, 619–627. doi:10.1002/1439-7633(20020703)3:7

Cai, W.-J., Huang, W.-J., Luther, G. W., Pierrot, D., Li, M., … Kemp, W. M. 2017 Redox reactions and weak buffering capacity lead to acidification in the Chesapeake Bay. *Nature Communications*, *8*, 369. doi:10.1038/s41467-017-00417-7

Carroll, A. R., Copp, B. R., Davis, R. A., Keyzers, R. A., & Prinsep, M. R. (2023). Marine natural products. *Natural Product Reports*, *40*, 275–325. doi:10.1039/D2NP00083K

Chaffin, J. D., Bridgeman, T. B., & Bade, D. L. (2013). Nitrogen constrains the growth of Late Summer cyanobacterial blooms in Lake Erie. *Advances in Microbiology*, *03*, 16–26. doi:10.4236/aim.2013.36A003

Che, Y., Ding, L., Qiu, J., Ji, Y., & Li, A. (2020). Conversion and Stability of New metabolites of Paralytic Shellfish toxins under different Temperature and pH Conditions. *Journal of Agricultural and Food Chemistry*, *68*, 1427–1435. doi:10.1021/acs.jafc.9b07063

Dunkel, M. (2006). SuperNatural: A searchable database of available natural compounds. *Nucleic Acids Research*, *34*, D678–D683. doi:10.1093/nar/gkj132

Ernst, M., Kang, K. B., Caraballo-Rodríguez, A. M., Nothias, L.-F., Wandy, J.,… van der Hooft, J. J. J. (2019). MolNetEnhancer: Enhanced Molecular Networks by Integrating Metabolome Mining and Annotation Tools. *Metabolites*, *9*(7), 144. doi:10.3390/metabo9070144

Falkenberg, L. J., Bellerby, R. G. J., Connell, S. D., Fleming, L. E., Maycock, B. … Dupont, S. (2020). Ocean acidification and human health. *International Journal of Environmental Research and Public Health*, *17*, 4563. doi:10.3390/ijerph17124563

Fu, W., Nelson, D. R., Mystikou, A., Daakour, S., & Salehi-Ashtiani, K. (2019). Advances in microalgal Research and engineering development. *Current Opinion in Biotechnology*, *59*, 157–164. doi:10.1016/j.copbio.2019.05.013

Horai, H., Arita, M., Kanaya, S., Nihei, Y., Ikeda, T., … Nishioka, T. (2010). MassBank: A public repository for sharing mass spectral data for life sciences. *Journal of Mass Spectrometry: JMS*, *45*, 703–714. doi:10.1002/jms.1777.

Hort, V., Abadie, E., Arnich, N., Bottein, M.-Y. D., & Amzil, Z. (2021). Chemodiversity of Brevetoxins and other potentially toxic metabolites produced by *Karenia* spp. and their metabolic products in marine organisms. *Marine Drugs*, *19*, 656. doi:10.3390/md19120656

Hwang, S.-W., Choi, H. I., & Sim, S. J. (2019). Acidic cultivation of *Haematococcus pluvialis* for improved astaxanthin production in the presence of a lethal fungus. *Bioresource Technology*, *278*, 138–144. doi:10.1016/j.biortech.2019.01.080

Liska, A. J., Shevchenko, A., Pick, U., & Katz, A. 2004 Enhanced photosynthesis and redox energy production contribute to salinity tolerance in *Dunaliella* as revealed by homology-based proteomics. *Plant Physiology*, *136*, 2806–2817. doi:10.1104/pp.104.039438

Li, J., Zhang, J., Huang, W., Kong, F., Li, Y., Xi, M., & Zheng, Z. (2016). Comparative bioavailability of ammonium, nitrate, nitrite and urea to typically harmful cyanobacterium *Microcystis aeruginosa*. *Marine Pollution Bulletin*, *110*, 93–98. doi:10.1016/j.marpolbul.2016.06.077

MarinLit. (2021). A database of the marine natural products literature. Retrieved from http://pubs.rsc.org/marinlit/

Mehar, M. U. N., Mudliar, J. G., Shekh, S. N., & Shekh, A. Y. (2019). Recent advances in microalgal bioactives for food, feed, and healthcare products: Commercial potential, market space, and sustainability. *Comprehensive Reviews In Food Science And Food Safety*, *18*, 1882–1897. doi:10.1111/1541-4337.12500

Morel, F. M. M., Rueter, J. G., Anderson, D. M., & Guillard, R. R. L. (1979). Aquil: a chemically defined phytoplankton culture medium for trace metal studies. *Journal of Phycology*, *15*, 135–141. doi:10.1111/j.1529-8817.1979.tb02976.x

Nagappan, S., Devendran, S., Tsai, P.-C., Jayaraman, H., Alagarsamy, V., Pugazhendhi, A., & Ponnusamy, V. K. (2020). Metabolomics Integrated with transcriptomics and proteomics: Evaluation of systems reaction to nitrogen deficiency stress in microalgae. *Process Biochemistry*, *91*, 1–14. doi:10.1016/j.procbio.2019.11.027

Nothias, L.-F., Nothias-Esposito, M., da Silva, R., Wang, M., Protsyuk, I. , and Dorrestein, P. C. (2018). Bioactivity-based molecular networking for the discovery of drug leads in natural product Bioassay-Guided Fractionation. *Journal of Natural Products*, *81*, 758–767. doi:10.1021/acs.jnatprod.7b00737

Nymark, M., Sharma, A. K., Sparstad, T., Bones, A. M., & Winge, P. (2016). A CRISPR/Cas9 system adapted for gene editing in marine algae. *Scientific Reports*, *6*, 24951. doi:10.1038/srep24951

Pacific Ocean | Depth. (2021). Temperature, Animals, Location, Map, & Facts. Retrieved from https://www.britannica.com/place/Pacific-Ocean.

Pluskal, T., Castillo, S., Villar-Briones, A., & Orešič, M. (2010). Mzmine 2: Modular framework for processing, visualizing, and analyzing mass spectrometry-based molecular profile data. *BMC Bioinformatics*, *11*, 395. doi:10.1186/1471-2105-11-395

Poliner, E., Pulman, J. A., Zienkiewicz, K., Childs, K., Benning, C., & Farré, E. M. (2018). A toolkit for *Nannochloropsis oceanica* CCMP 1779 enables gene stacking and genetic engineering of

the eicosapentaenoic acid pathway for enhanced Long - chain polyunsaturated fatty acid production. *Plant Biotechnology Journal*, *16*, 298–309. doi:10.1111/pbi.12772

Renaud, S. M., & Parry, D. L. (1994). Microalgae for use in tropical aquaculture II: Effect of salinity on growth, gross chemical composition and fatty acid composition of three species of marine microalgae. *Journal of Applied Phycology*, *6*, 347–356. doi:10.1007/BF02181949

Shannon, P., Markiel, A., Ozier, O., Baliga, N. S., Wang, J. T., Ramage, D., & Schwikowski, B. (2003). Cytoscape: A software environment for integrated models of biomolecular interaction networks. *Genome Research*, *13*, 2498–2504. doi:10.1101/gr.1239303

Smayda, T. J. (2008). Complexity in the eutrophication–harmful algal bloom relationship, with comment on the importance of grazing. *Harmful Algae*, *8*, 140–151. doi:10.1016/j.hal.2008.08.018

Tett, P., Droop, M. R., & Heaney, S. I. (1985). The Redfield ratio and phytoplankton growth rate. *Journal of the Marine Biological Association of the United Kingdom*, *65*, 487–504. doi:10.1017/S0025315400050566

Teuma, L., Sanz-Luque, E., Guieysse, B., & Plouviez, M. (2023). Are microalgae new players in nitrous oxide emissions from eutrophic aquatic environments? *Phycology*, *3*, 356–367. doi:10.3390/phycology3030023

Wandy, J., Zhu, Y., van der Hooft, J. J. J., Daly, R., Barrett, M. P., & Rogers, S. M. O. (2018). Web-based topic modelling for substructure discovery in mass spectrometry. *Bioinformatics*, *34*, 317–318. doi:10.1093/bioinformatics/btx582

Wang, M., Carver, J. J., Phelan, V. V., Sanchez, L. M., Garg, N. . . . Bandeira, N. (2016). Sharing and community curation of mass spectrometry data with global natural products social molecular networking. *Nature Biotechnology*, *34*, 828–837. doi:10.1038/nbt.3597

Xi, Y., Kong, F., & Chi, Z. (2021). ROS induce β-carotene biosynthesis caused by changes of photosynthesis efficiency and energy metabolism in *Dunaliella salina* under stress conditions. *Frontiers in Bioengineering and Biotechnology*, *8*, 613768. doi:10.3389/fbioe.2020.613768

Xu, Y., & Harvey, P. J. (2019). Carotenoid production by *Dunaliella salina* under red light. *Antioxidants*, *8*, 123. doi:10.3390/antiox8050123